Solvent Effects on Internal Conversions and Intersystem Crossings: The Radiationless De-Excitation of Acrolein in Water

Aurora Muñoz Losa, Ignacio Fdez. Galván, M. Luz Sánchez, M. Elena Martín, and Manuel A. Aguilar*

Química Física, Universidad de Extremadura, Avda. de Elvas s/n 06071 Badajoz, Spain

Received: July 20, 2007; In Final Form: October 9, 2007

An extended version of the averaged solvent electrostatic potential from molecular dynamics data (ASEP/MD) method oriented to the study of the solvent effects on internal conversion and intersystem crossing processes is presented. The method allows for the location of crossing points between free energy surfaces both in equilibrium and in frozen solvent conditions. The ground and excited states of the solute molecule are described at the complete active space self-consistent field (CASSCF) level while the solvent structure is obtained from molecular dynamics simulations. As an application, we studied the nonradiative de-excitation of s-*trans*-acrolein $^1(n \rightarrow \pi^*)$ in aqueous solution. We found that the solvent modifies the relative stability of the different crossing points but not enough as to alter the relative order of stability with respect to the in vacuo situation. The relaxation through an equilibrium path involves a strong solvent reorganization. On the contrary, the nonequilibrium path does not involve solvent motion and the de-excitation could proceed with the same speed as in vacuo.

I. Introduction

It is well-known that solvent effects play a fundamental role in chemistry. The solvent affects the kinetics and thermodynamics of chemical reactions, modifying the nature and ratio of the products, it also modifies the appearance of spectra, shifting the position of bands or modifying their intensities. In the past decades, much effort has been dedicated to the development of models allowing the study of solvent effects on chemical equilibrium and reactions and molecular spectra. Comparatively, less attention has been paid, however, to the study of solvent effects on the evolution and reactivity of molecules in excited states, that is, photophysical and photochemical processes. The reasons are obvious, to the difficulties inherent to the study of nonadiabatic processes[1,2] (processes that imply more than one potential energy surface) in vacuo, one must add the complications associated to the presence of a solvent, that is, the existence of a manifold of configurations thermally accessible that must be included to obtain statistically significant results and the great number of solvent molecules that interact with the solute molecule.

One can distinguish two basic types of crossing points between potential energy surfaces: conical intersection (CI) if the crossing is between states with the same spin symmetry, giving rise to internal conversion (IC) processes, or singlet−triplet crossing (STC), for instance, if the states have different spin symmetry, and this leads to intersystem crossing (ISC). The work developed by the groups of Yarkony,[3] Ruedenberg et al.,[4] and Robb et al.[5] has shown that CI and STC are a very common feature of potential energy surfaces. As a result of that, presently, one can use techniques and algorithms that permit the determination of those geometries for which CI and STC appear for in vacuo systems. The extension of these techniques to in-solution systems is not easy because the methods must permit (a) the inclusion of the solvent effects on the energy, wave functions, and gradients (ground and excited states, derivative coupling) of the solute used by the CI and STC searching algorithms in solution and (b) the calculation of the free energy differences between the different structures (CI, STC, minima, Franck−Condon (FC) points) involved in the photochemical process.

Furthermore, in solution, there exists a subtle interplay between the dynamics of the solvent and the time evolution of the excited state. A photochemical process begins usually with the excitation from the minimum energy configuration of the ground state to the Franck−Condon point on the excited-state free energy surface. In solution, in the FC point, the solvent is in a nonequilibrium situation, that is, the solvent structure corresponds to the equilibrium with the solute ground state and not with the actual solute charge distribution in the excited state. As time goes on, the solvent modifies its structure, and after a long enough time, it becomes equilibrated with the charge distribution of the solute excited state. In the photochemistry of in-solution systems, we can hence define two limiting situations depending on whether the solvent is in an equilibrium or nonequilibrium situation. Most theoretical models proposed to date have considered nonequilibrium solvation. The consideration of nonequilibrium solvation is motivated by the fact that most radiationless relaxations take place on the femtosecond time scale, a scale in which, probably, the solvent equilibration is not complete. However, in systems where the geometry of the CI or STC points involved in the photochemical process are very different from the FC point, the reaction will take place only after a great part of the solvent reorganization has occurred.

A few recent studies have proposed methods to include solvent effects in the study of IC processes. Burghardt et al.,[6,7] for instance, use continuum methods to study IC in solution; these authors introduce an explicit coordinate for the solvent, which permits them to study the solvation dynamics during the internal conversion process. Methods that permit a more detailed description of the solvent have also been proposed; therefore,

* Corresponding author. E-mail: maguilar@unex.es.

10.1021/jp075706v CCC: $40.75
Published on Web 12/22/2007

in a recent paper, Yamazaki and Kato[8] use the RISM-SCF method for describing the solvent dynamics during energy surface crossing in ethylene and $CH_2NH_2^+$ in polar solvents. Finally, several groups[9−11] have used quantum mechanics/molecular mechanics (QM/MM) methods to locate CI generally in nonequilibrium conditions, that is, for a frozen solvent structure.

In this paper, we present an extension of a sequential QM/MM method that permits us to locate and describe the energetic and geometrical properties of unavoided crossings of potential energy surfaces in solution both in equilibrium and in nonequilibrium conditions. The proposed method is an extension to the case of solvated molecules of an algorithm due to Bearpark et al.[12] The method is valid for all types of crossings and combines a high level ab initio quantum-mechanical description of the solute with a detailed description of the solvent obtained through molecular dynamics (MD) simulations.

We apply the proposed method to the study of the different ICs and ISCs involved in the radiationless relaxation of s-*trans*-acrolein. Acrolein or propenal is the smallest α,*β*-unsaturated carbonyl compound. The interaction between the carbonyl group and the C═C double bond makes it a compound of marked interest from a spectroscopic and photochemical point of view. Furthermore, it has been shown that it can form several hydrogen bonds with the water molecules, a situation where the employment of simplified solvent models, such as dielectric continuum models, is not adequate. The photochemistry of this compound has already been studied in gas-phase conditions.[5a] However, to our knowledge, no intent has been done for including the solvent effects.

The rest of the paper is organized as follows: section II explains the algorithms to locate and characterize the CI and STC points in solution. Section III describes the computational details of the study. Section IV discusses the influence of the solvent on the position and features of the different CIs and STCs in s-*trans*-acrolein. Finally, section V states the main conclusions of the study.

II. Method

In the description of the solvent effects, we used the averaged solvent electrostatic potential from molecular dynamics data (ASEP/MD) method[13−14] developed in our laboratory. ASEP/MD is a QM/MM effective Hamiltonian method that makes use of the mean field approximation.[13d] In this approximation, the average value of any solute property is replaced by the value calculated in the presence of an average perturbation or configuration. The method combines quantum mechanics (QM) and molecular dynamics (MD) techniques, with the particularity that full QM and MD calculations are alternated and not simultaneous. During the MD simulations, the intramolecular geometries and charge distributions of all molecules are considered as fixed. From the resulting data, the average electrostatic potential generated by the solvent on the solute is obtained. This potential is introduced as a perturbation into the solute's quantum mechanical Hamiltonian, and by solving the associated Schrödinger equation, one gets a new charge distribution for the solute, which is used in the next MD simulation. The iterative process is repeated until the electron charge distribution of the solute and the solvent structure around it are mutually equilibrated. The main characteristics of the method have been described elsewhere.[13−14] Here, we shall detail only some points pertinent to the current study.

In ASEP/MD the energies, *E*, and electronic wave functions, Ψ, of the solute molecule in presence of the average perturbation generated by the solvent are obtained by solving an effective Schrödinger equation

$$(\hat{H}_{QM} + \hat{H}_{QM/MM})|\Psi\rangle = E|\Psi\rangle \quad (1)$$

where $\hat{H}_{QM}$ is the "in vacuo" solute molecular Hamiltonian and where the solute−solvent interaction term, $\hat{H}_{QM/MM}$ takes the following form:

$$\hat{H}_{QM/MM} = \hat{H}^{elect}_{QM/MM} + \hat{H}^{vdw}_{QM/MM} \quad (2)$$

$$\hat{H}^{elect}_{QM/MM} = \int d\mathbf{r}\cdot\hat{\rho}\cdot\langle V_S(r;\rho)\rangle \quad (3)$$

where $\hat{\rho}$ is the solute charge density operator and the brackets denote a statistical average. The term $\langle V_S(r;\rho)\rangle$ is the averaged electrostatic potential generated by the solvent at the position *r* and is obtained from MD calculations where the solute molecule is represented by the charge distribution ρ and a geometry fixed during the simulation. For details about the calculation of $\langle V_S(r;\rho)\rangle$, see ref 14. The $\hat{H}^{vdw}_{QM/MM}$ term is the Halmiltonian for the van der Waals interaction, in general, represented by a Lennard-Jones potential. This term is calculated by averaging its value over all solvent configurations selected during the MD simulation. It depends only on the nuclear coordinates and hence has no effect on the solute wave function, but it contributes to the final value of the energy, gradient, and Hessian.

To locate a minimum energy crossing point, we have combined the ASEP/MD method with an algorithm due to Bearpark et al.,[12] which permits to locate the minimum energy point of the CI (MECI) or STC (MESTC) seam without employing Lagrange multipliers. This algorithm simultaneously minimizes the energy difference between the two intersecting states and the energy of the crossing seam between the two potential energy surfaces.[10] The final form taken by the gradient is:

$$\vec{f}_{KL} = 2(E_K - E_L)\hat{g}_{KL} + [\nabla E_K - (\nabla E_K\cdot\hat{g}_{KL})\hat{g}_{KL} - (\nabla E_K\cdot\hat{h}_{KL})\hat{h}_{KL}] \quad (4)$$

here, E_K and E_L are the energies of the intersecting surfaces, ∇E_K is the gradient of the upper state and $\hat{g}_{KL}$ and $\hat{h}_{KL}$ are the two versors that define the branching space or $g-h$ plane,[1] that is, the subspace of nuclear coordinates in which the degeneracy between the two intersecting surfaces is lifted linearly in displacements from the intersection. When the two intersecting states have different spin symmetry as in the case of STC, the $\hat{h}_{KL}$ term vanishes, and only one coordinate defines the branching space. The expression taken by the gradient difference vector ($\vec{g}_{KJ}$) is:

$$\vec{g}_{KL} = \nabla(E_K - E_L) \quad (5)$$

and the derivative coupling vector ($\vec{h}_{KL}$):

$$\vec{h}_{KL} = \langle\Psi_K|\nabla|\Psi_L\rangle \quad (6)$$

where the gradient ∇ is a vector in the nuclear space and Ψ_1 are the adiabatic electronic wave functions, eigenfunctions of the electronic Hamiltonian, $\hat{H}$, with energies E_i. The corresponding versors are defined as $\hat{g}_{KL} = \vec{g}_{KL}/|\vec{g}_{KL}|$ and $\hat{h}_{KL} = \vec{h}_{KL}/|\vec{h}_{KL}| - [(\vec{h}_{KL}/|\vec{h}_{KL}|)\hat{g}_{KL}]\hat{g}_{KL}$.

In the definition of the gradient $\vec{f}_{KL}$, eq 4, the solvent can affect (1) the energy difference between the two states E_K and E_L, (2) the gradient of the upper excited state, ΔE_K, and (3)

the two vectors that define the branching space, $\hat{g}_{KL}$ and $\hat{h}_{KL}$. Next, we analyze in detail the solvent influence on each one of these terms.

(1) Energy Difference, ($E_K - E_L$).

$$(E_K - E_L) = \langle \Psi_K | \hat{H}_{QM} + \hat{H}_{QM/MM} | \Psi_K \rangle - \langle \Psi_L | \hat{H}_{QM} + \hat{H}_{QM/MM} | \Psi_L \rangle \quad (7)$$

E and Ψ are obtained by solving eqs 1−3. The interaction term is the sum of the electrostatic and van der Waals contributions. In turn, the electrostatic contribution can be split into two components: the interaction between solute nuclei and solvent charges, $\hat{H}^{elect,n}_{QM/MM}$, and the interaction between the solute electronic charge distribution and the solvent charges, $\hat{H}^{elect,e}_{QM/MM}$

$$\begin{aligned}(E_K - E_L) = {} & \langle \Psi_K | \hat{H}_{QM} | \Psi_K \rangle - \langle \Psi_L | \hat{H}_{QM} | \Psi_L \rangle + \\ & \langle \Psi_K | \hat{H}^{elect,n}_{QM/MM} | \Psi_K \rangle - \langle \Psi_L | \hat{H}^{elect,n}_{QM/MM} | \Psi_L \rangle + \\ & \langle \Psi_K | \hat{H}^{elect,e}_{QM/MM} | \Psi_K \rangle - \langle \Psi_L | \hat{H}^{elect,e}_{QM/MM} | \Psi_L \rangle + \\ & \langle \Psi_K | \hat{H}^{vdw}_{QM/MM} | \Psi_K \rangle - \langle \Psi_L | \hat{H}^{vdw}_{QM/MM} | \Psi_L \rangle \quad (8)\end{aligned}$$

In this point, we introduce the following approximation: we suppose that the Lennard-Jones coefficients are the same for all of the electronic states of a molecule. Furthermore, taking into account the fact that the two states K and L are calculated at the same geometry, one can simplify eq 8 and obtain the final expression for the energy difference:

$$\begin{aligned}(E_K - E_L) = {} & \langle \Psi_K | \hat{H}_{QM} | \Psi_K \rangle - \langle \Psi_L | \hat{H}_{QM} | \Psi_L \rangle + \\ & \langle \Psi_K | \hat{H}^{elect,e}_{QM/MM} | \Psi_K \rangle - \langle \Psi_L | \hat{H}^{elect,e}_{QM/MM} | \Psi_L \rangle \quad (9)\end{aligned}$$

The energy difference depends implicitly on the solvent through the in-solution wavefunctions Ψ_K and Ψ_L and explicitly through the $\hat{H}^{elect,e}_{QM/MM}$ terms.

(2) Upper State Gradient, ∇E_K. In the calculation of this gradient, we use a variant of the free energy gradient method[15] described in a previous paper. The gradients at the point r of the free energy surface E_K are calculated as:[13d]

$$\begin{aligned}\nabla E_K(r) = \frac{\partial G_K(r)}{\partial r} = \left\langle \frac{\partial H_K(r, X)}{\partial r} \right\rangle \approx {} & \frac{\partial \langle H_{QM}(r, X) \rangle}{\partial r} + \\ & \frac{\partial \langle H^{elect}_{QM/MM}(r, X) \rangle}{\partial r} + \left\langle \frac{\partial H^{vdw}_{QM/MM}(r, X)}{\partial r} \right\rangle \quad (10)\end{aligned}$$

where the brackets denote a statistical average over the solvent configurations, X. As we can see, electrostatic and van der Waals contribution are calculated in a different way. In the case of the electrostatic term, the gradient is calculated as the gradient of an averaged solvent configuration; however, the van der Waals contribution is calculated as the averaged value of the gradients of all solvent configurations selected.

(3) Gradient Difference ($\vec{g}_{KL}$) and Derivative Coupling ($\vec{h}_{KL}$) Vectors. By differentiating eq 9, one obtains:

$$\begin{aligned}\vec{g}_{KL} = \nabla(E_K - E_L) = \nabla E_K - \nabla E_L = {} & \nabla[\langle \Psi_K | \hat{H}_{QM} | \Psi_K \rangle - \\ & \langle \Psi_L | \hat{H}_{QM} | \Psi_L \rangle] + \nabla[\langle \Psi_K | \hat{H}^{elect,e}_{QM/MM} | \Psi_K \rangle - \langle \Psi_L | \hat{H}^{elect,e}_{QM/MM} | \Psi_L \rangle] \quad (11)\end{aligned}$$

where the van der Waals and nuclear terms vanish because they depend only on nuclear coordinates and hence take the same values for all the electronic states. (Note that in those cases where the Hellmann−Feynman theorem is applicable the last term of the right hand side (rhs) of eq 11 vanishes because the $\hat{H}^{elect,e}_{QM/MM}$ operator does not depend explicitly on the nuclear coordinates of the solute.)

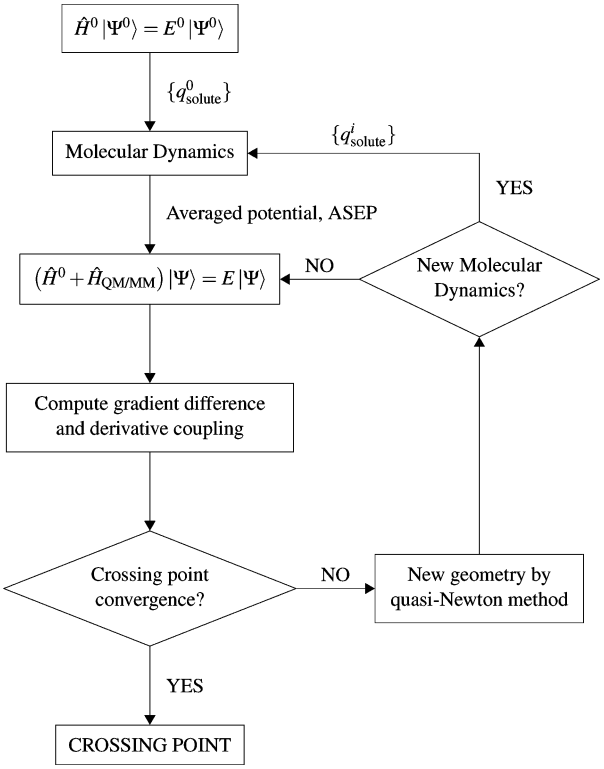

Figure 1. CI and STC points location scheme.

In the calculation of the derivative coupling, eq 6 is used with the solute wave function perturbed by the solvent.

The complete scheme of the process followed to locate CI or STC points of molecules in solution using ASEP/MD is shown in Figure 1. We begin by equilibrating the solvent and the solute charge distribution at the ground state and getting a set of point charges that represent the in-solution charge distribution of the solute molecule in the ground state. In our case, these charges are usually obtained using the CHELPG method.[16] These charges are then used as input for an MD simulation of the solute and solvent molecules, the remaining solute (LJ coefficients) and solvent (charges and LJ coefficients) parameters are obtained from the literature. N representative solvent configurations (N usually taken between 500 and 1000) are selected from the MD simulation. From these configurations, the averaged solvent potential, eq 3, generated by the solvent in the volume occupied by the solute is calculated. Next, the electronic Schrödinger equation, eq 1, for the solute molecule is solved in the presence of the averaged perturbation generated by the solvent. The energies and wave functions of the crossing states together with the rest of terms appearing in eqs 4−11 are calculated, and the gradient $\vec{f}_{KL}$ is obtained. A new solute geometry is estimated by using a quasi-Newton method. In this point, we have two possibilities depending on whether the solvent is in an equilibrium or frozen solvent situation. In the former case, the solvent must be equilibrated with the solute charge distribution of the upper state and hence a new MD must be performed; the procedure is continued until the solvent distribution and the charge distribution of the upper state are mutually equilibrated. The choice of the upper state is justified by the physical process of de-excitation, where the system evolves in the excited-state surface and the involved crossing points are those where the solvent is in equilibrium with this excited state (within the equilibrium approximation). Although

strictly speaking, it would be necessary to perform an MD simulation for each new solute geometry; this is a very inefficient procedure. It has been verified that it is computationally more efficient to perform several steps of the CI or STC search procedure before equilibrating again the solvent. We update the solvent structure only after 10−20 iterations of the crossing point search procedure.

In the case of frozen conditions, the CI or STC points are located for a fixed solvent structure. During an electron transition, the Franck−Condon principle is applicable, and the solvent nuclei remain fixed. Consequently, the solvent structure is in equilibrium with the charge distribution of the solute ground state. The crossing point search procedure is performed in the presence of this solvent structure.

Once the different CI and STC have been located, it is necessary to determine their relative stabilities. For in-solution systems, the relevant quantity is the free energy difference. The standard free-energy difference between the initial and the final state in solution, a CI and a minimum or FC point, for instance, can be written as the sum of two terms:[17]

$$\Delta G_{\text{diff}} = \Delta E_{\text{solute}} + \Delta G_{\text{int}} \tag{12}$$

where

$$\Delta E_{\text{solute}} = E^f - E^i = [\langle \Psi^f | \hat{H}_{\text{QM}} | \Psi^f \rangle - \langle \Psi^i | \hat{H}_{\text{QM}} | \Psi^i \rangle] \tag{13}$$

is the ab initio energy difference between the two quantum mechanics, QM, states calculated using the in vacuo solute molecular Hamiltonian, $\hat{H}_{\text{QM}}$, and the in-solution wavefunctions, and ΔG_{int} is the difference in the solute−solvent interaction free energy between the two QM states. The free-energy perturbation method[18] was used to determine this energy. The solute geometry was assumed to be rigid and a function of the perturbation parameter (λ) while the solvent was allowed to move freely. When $\lambda = 0$, the solute geometry and charges correspond to the initial state. When $\lambda = 1$, the charges and geometry are those of the final state. For intermediate values, a linear interpolation is applied. A value of $\Delta\lambda = 0.05$ was used. That means that a total of 21 separate molecular dynamics simulations were carried out to determine the free energy difference. To test the convergence of the calculation, the difference in interaction free energies calculated forward and backward was compared. In order to clarify the role played by the solvent in the stabilization of the different structures, it is useful to split the ΔG_{int} term into two components, $\Delta G_{\text{int}} = \Delta E_{\text{int}} + \Delta G_{\text{solv}}$. The last term, ΔG_{solv}, provides the solvent distortion energy, that is, the energy spent in changing the solvent structure from an initial to a final state. The term ΔE_{int}, accounts for the difference in the solute−solvent interaction energy between the final and the initial state.

III. Computational Details

We have studied the CI and STC points involved in the radiationless de-excitation of s-*trans*-acrolein in aqueous solution considering equilibrium and nonequilibrium conditions for the solvent. The states were described using the CASSCF level of theory. The active space was spanned by all of the configurations arising from six valence electrons in five orbitals (6e/5o). All the calculations were performed with the ASEP/MD program[13a] using the data provided by Gaussian 98[19] and Moldy[20] and the 6-31G* basis set. The initial geometry for acrolein was obtained by CASSCF optimization both in vacuum and in solution with the aforementioned basis set. In all cases, we take as initial point of the CI search procedure the geometry of the Franck−Condon (FC) excitation, that is, the geometry of the ground state minimum.

TABLE 1: Energy Results in au, ΔE and ΔG in kcal/mol

		vacuum		solution		
		E	ΔE	ΔG eq.	ΔE non-eq.	geometry
S_1	FC	−190.6788	0.0	0.0	0.0	
S_0	min	−190.8235	−90.8	−95.8		planar
S_1	min	−190.7081	−18.4	−20.7		planar
T_2	min	−190.7131	−21.5	−22.3		planar
T_1	min	−190.7278	−35.7	−36.4		twisted
S_1/T_1	STC	−190.7044	−16.1	−19.2	−17.7	planar
T_2/T_1	CI	−190.7055	−16.7	−19.1	−18.4	planar
T_1/S_0	STC	−190.7275	−30.5	−33.7	−34.2	twisted
S_1/S_0	CI	−190.6762	+1.6	−1.4	+6.4	twisted

To locate the CI or STC point, we used a quasi-Newton method where the increment of geometry h is defined by

$$h = -\sum_{i=1}^{n} \frac{\vec{v}_i^{\,t} \vec{f}_{KL} \vec{v}_i}{b_i} \tag{14}$$

Here, $\vec{v}_i$ and b_i are the eigenvectors and the eigenvalues, respectively, of the Hessian matrix and f_{KL} the gradient described previously. To update the approximate Hessian, we employed the Broyden−Fletcher−Goldfarb−Shanno (BFGS) algorithm. We consider that the CI or STC point has been reached when the energy difference between the two states is lower than 0.002 au (∼1.3 kcal/mol) and the energy and geometry are stabilized. The minimal energy CI (MECI) or STC (MESTC) is the lowest energy point that fulfills these conditions. In solution, the results are affected by statistical uncertainty, and we take average values of the last 5 ASEP/MD cycles.

A total of 251 molecules were simulated with fixed intramolecular geometry by combining LJ interatomic interactions with electrostatic interactions. The solvent was represented by 250 TIP3P[21,22] molecules in a cubic box of 18.7 Å side. Periodic boundary conditions were applied, and spherical cutoffs were used to truncate the molecular interactions at 9.0 Å. A time step of 0.5 fs was used. The electrostatic interaction was calculated with the Ewald method. The temperature was fixed at 298 K by using a Nosé-Hoover thermostat. Each MD calculation simulation was run for 75 ps (25 ps equilibration, 50 ps production).

IV. Results

In the radiationless relaxation of acrolein, there are at least four states involved: the ground state, S_0, the first singlet excited state, $S_1(n \rightarrow \pi^*)$, and two triplet states, $T(\pi \rightarrow \pi^*)$ and $T(n \rightarrow \pi^*)$. Given that there are several surface crossings, the relative order of the states depends on the geometry of the molecule. For a given multiplicity, we classify the states T_1, T_2, and so forth, according to the order of stability of their absolute minima; see Table 1. So, we denote as T_1 the $T(\pi \rightarrow \pi^*)$ state and as T_2 the $T(n \rightarrow \pi^*)$ state.

Two paths have been proposed in order to explain the radiationless de-excitation of acrolein in gas phase: (1) a direct de-excitation through a S_1/S_0 IC and (2) an indirect path that starts with a S_1/T_1 ISC. From here, we have several possibilities: (a) the system can return to the ground state through a T_1/S_0 ISC or (b) the system can pass to T_2 through a T_1/T_2 IC. From T_2, acrolein can relax radiatively (giving rise to a very weak band in the phosphorescence spectrum), or it can return to T_1 and from here to S_0 through an ISC, as in possibility (a).

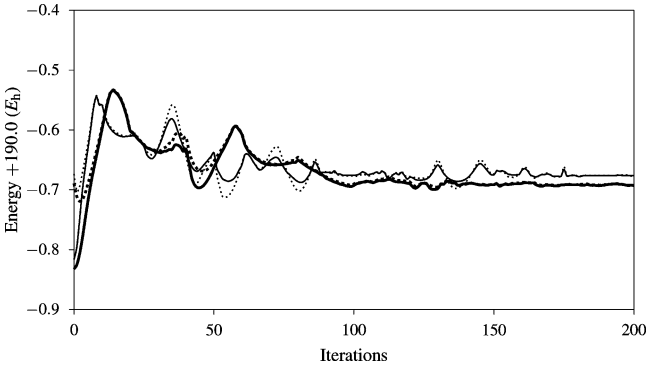

Figure 2. Evolution during the search procedure of the S_0 and S_1 energies (in hartree) in vacuum (thin lines, continuous and dotted, respectively) and in solution (thick lines, continuous and dotted, respectively).

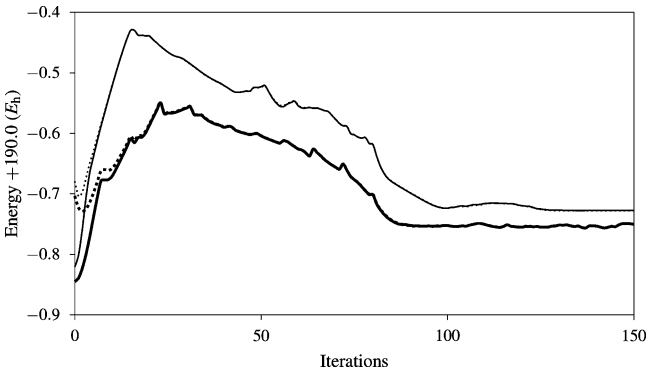

Figure 3. Evolution during the search procedure of the S_0 and T_1 energies (in hartree) in vacuum (thin lines, continuous and dotted, respectively) and in solution (thick lines, continuous and dotted, respectively).

The main objective of this paper is to determine if this scheme is also valid when the system is in aqueous solution. Furthermore, we will try to clarify the solvent's influence on the geometry and relative stability of the different crossing points and states involved and the role of the solvent dynamics (equilibrium solvation or frozen solvent) in the acrolein relaxation.

Figures 2 and 3, display the evolution of the total energy in vacuo and in solution as a function of the number of cycles of the search procedure. Figure 2 represents the search of the S_1/S_0 CI point, and Figure 3 represents the corresponding to the T_1/S_0 STC. In the first steps, the energy difference between the two crossing states decreases until the system is close to the CI or STC seam. Then the energy decreases until the MECI or MESTC is reached. Each time a new MD is performed, the solvent structure is recalculated. If the structure change is important, the position of the crossing seam changes, and the energies begin to fluctuate until they are again stabilized in a new plateau. The in-solution values (energies, geometries, dipoles, etc.) are calculated by averaging over the results obtained with the last 5 cycles of the ASEP/MD process.

The main results obtained in this paper are displayed in Table 1 and Figure 4. Table 1 provides the relative stability of the different minima, CI and STC points, calculated in vacuo and in solution, and in this latter case, in equilibrium and frozen solvent conditions. Figure 4 displays the geometries of the minima and minimal energy CI and STC.

We begin by analyzing the influence of the solvent on the different geometries supposing solvent equilibrium conditions. In all the cases analyzed, minima, MECI and MESTC, the solvent increases the CO distance and decreases the two CC distances with respect to the in vacuo values. This behavior can be explained by the formation of hydrogen bonds between the carbonyl oxygen and the hydrogen of the water molecules. The largest distance variations appear in the T_1/S_0 STC and T_1/T_2 CI. The variation of the geometrical parameters does not correlate with the induced dipole moment (see Table 2). In fact, the largest values of the induced dipole moments are obtained for the S_1/S_0 CI and T_1 minimum. In order to explain the variation of the geometrical and electric properties, it is necessary to consider two variables: the bond order of the carbonyl group and the in vacuo dipole moment value. The largest variations of the dipole moment appear in those structures where the CO bond retains its double bond character. The solvent stabilizes the zwitterionic form of the double bond through the formation of hydrogen bonds and hence increases the dipole moment. On the contrary, the largest variations of distances appear in those structures where the CO bond has a single bond character and the dipole moment is high. In these conditions, the bond is more labile and hence easier to elongate. In twisted structures, the solvent affects slightly the $C_1C_2C_3H_3$ torsion angle value, which, in the S_1/S_0 CI structure, for instance, increases from 100° to 103°.

The solvent has also effects on the relative energies of the minima and crossing points, Table 1. All data have been referred to the FC points (in vacuo and in solution) which are the points where the de-excitation process initiates. We analyze first the solvent in equilibrium situation. Since the energies are referred to the FC point, the difference between the ground state energy in vacuo and that in solution provides the solvent shift of the $^1(n \rightarrow \pi^*)$ absorption band. The calculated solvent shift is 5.0 kcal/mol, very close to the experiment[23] (4.5 kcal/mol). As a general rule and when compared with the in vacuo values, the solvent stabilizes all of the minima and crossing points of acrolein. Within our approximation, in the FC point, the solvent is frozen, however in the rest of the points, minima, CI and STC, the solvent is in equilibrium with the corresponding solute charge distribution. The relaxation of the solvent from a nonequilibrium situation to an equilibrium situation explains the additional stabilization obtained in solution with respect to the in vacuo values. This is corroborated by the fact that all ΔG_{solv} values in Table 3 are negative. This table displays the values of the different contributions to ΔG. The solute−solvent interaction energy can sometimes take positive values; however, even in these cases, this energy is compensated by the energy gained during the relaxation of the solvent, given by ΔG_{solv}. A point to emphasize is that, except in the S_1/S_0 CI, in the rest of cases, the main contribution to ΔG_{diff} comes from ΔE_{solute}, that is, the relaxation of the solute geometry. It is this component which determines the relative stability order of the different excited states.

The main conclusion that one can obtain from Table 1 is that, in solution, the radiationless relaxation can follow the same path as in vacuo. The direct de-excitation, path 1 (see above), through the S_1/S_0 CI is unlikely but possible; it is 1.6 kcal/mol above the gas-phase FC point but 1.3 kcal/mol below the FC point in solution. However, this path involves an appreciable reorganization of the solvent structure, as is evidenced by the comparison between the OO and the OH radial distribution functions for the S_1/S_0 CI (dotted line in Figures 5 and 6) and FC point. Like for the gas-phase process, the most probable de-excitation path passes through the S_1/T_1 STC. This path implies also a large reorganization of the solvent structure around acrolein, and hence, given the larger times of relaxation

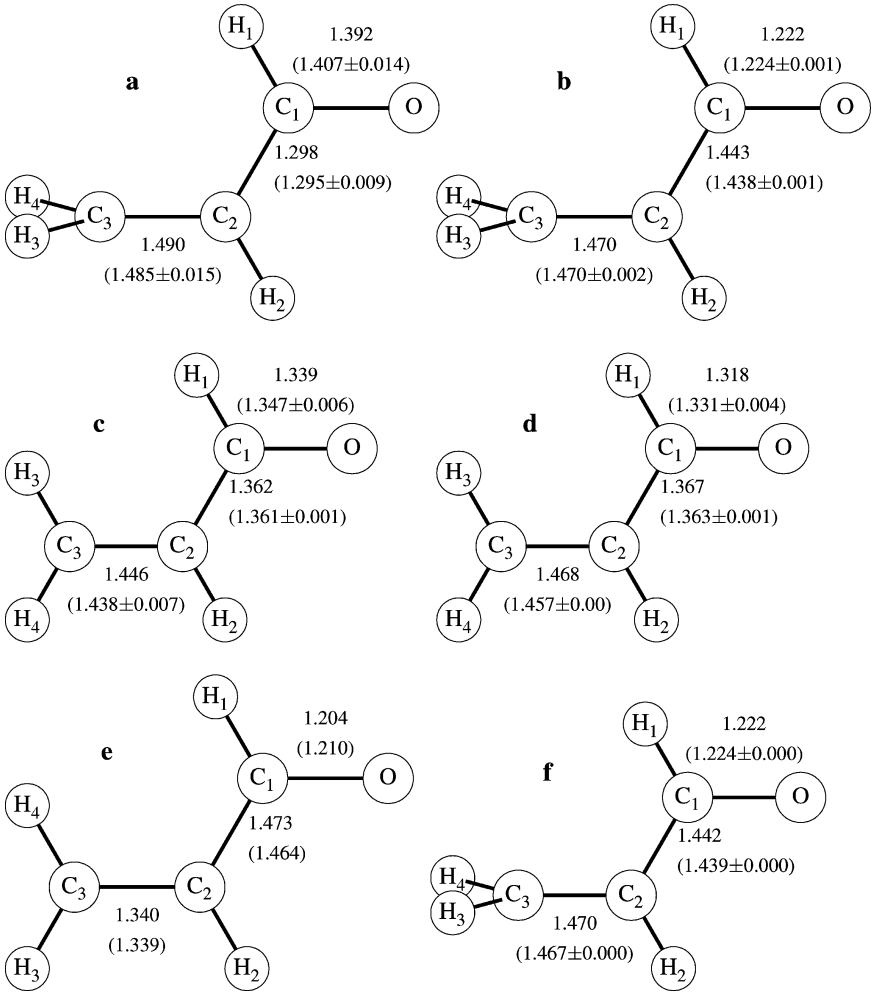

Figure 4. (a) S_1/S_0 CI geometry in vacuo and in solution (in parentheses). (b) T_1/S_0 STC geometry in vacuo and in solution (in parentheses). (c) S_1/T_1 STC geometry in vacuo and in solution (in parentheses). (d) T_1/T_2 CI geometry in vacuo and in solution (in parentheses). (e) FC geometry in vacuo and in solution (in parentheses). (f) T_1 minimum geometry in vacuo and in solution (in parentheses). Distances in Å.

TABLE 2: Dipole Moment Values in Debyes

		vacuum	solution	
			eq.	non-eq.
S_0	min	2.88	3.94 ± 0.04	
S_1	min	1.55	1.84 ± 0.08	
S_1	FC	1.05		1.87
T_2 $^3(n\rightarrow\pi^*)$	min	1.40	1.69 ± 0.03	
T_1 $^3(\pi\rightarrow\pi^*)$	min	2.88	3.90 ± 0.11	
S_1/T_1				
	S_1	1.41	1.70 ± 0.01	2.47
	T_1	2.45	2.93 ± 0.13	3.36
T_2/T_1				
	T_2	1.34	1.75 ± 0.13	1.34
	T_1	2.52	2.83 ± 0.09	2.52
T_1/S_0				
	T_1	2.90	3.91 ± 0.09	2.90
	S_0	2.87	3.85 ± 0.03	2.87
S_1/S_0				
	S_1	2.59	3.06 ± 0.05	2.78
	S_0	1.78	2.13 ± 0.08	3.60

of the solvent with respect to the relaxation times of the solute, one can expect equilibrium paths to be slower in solution than in vacuo.

The change of solvent structure around the solute depends on the nature of the excited-state considered; see Figures 5−7. The initial structure corresponds to the FC point, that is, to a solvent in equilibrium with the charge distribution of S_0 state. In this state, there is a strong interaction between the carbonyl group and the water molecules; the coordination number is close to 2. Regarding the solvent structure around the solute when this is in its singlet and triplet excited states, it depends on the type of transition involved. In $n \rightarrow \pi^*$ transitions, an electron is transferred from the oxygen lone pair to the carbon skeleton. As a consequence, the water−acrolein hydrogen bond weakens, and the first peak of both OO and OH radial distribution function (rdf) is shifted outward at the same time as its height decreases. The passing from the FC point to the final S_1/S_0 CI implies a partial desolvation of the carbonyl group, in fact, the coordination number decreases to 0.65. On the contrary, a $\pi \rightarrow \pi^*$ transition does not affect the strength of the hydrogen bond, and its effect on the solvent structure is smaller.

TABLE 3: Relative Free Energy (in kcal/mol) and Its Components in Different Points in Solution in Equilibrium Conditions

		ΔE_{solute}	ΔG_{solv}	ΔE_{int}	ΔG_{diff}
S_1	FC	0.0	0.0	0.0	0.0
S_1/T_1	STC	−16.5	−5.0	+2.3	−19.2
T_2/T_1	CI	−16.2	−4.5	+1.6	−19.1
T_1/S_0	STC	−28.0	−0.4	−5.3	−33.7
S_1/S_0	CI	+1.6	−7.0	+4.0	−1.4

Another point to emphasize is that the T_1/S_0 STC is very close in energy and geometry to the minimum of the T_1 state, consequently, the emission probability from this state must be very low. The weak phosphorescence band must be hence associated to the de-excitation from the T_2 state. In vacuo, the

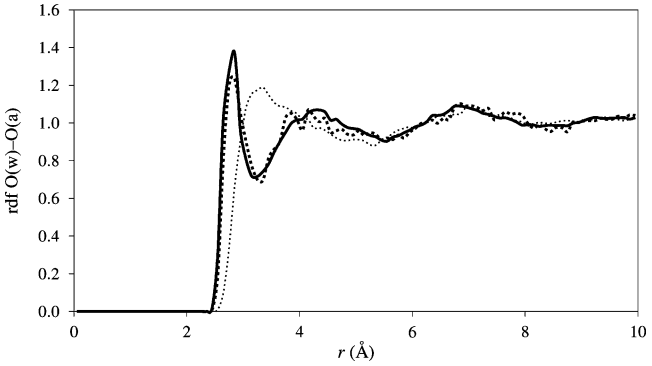

Figure 5. Oxygen(acrolein)−oxygen(water) radial distribution functions for S_0 minimum, T_1/S_0 STC (thick lines, continuous and dotted, respectively), and S_1/S_0 CI (thin dotted line).

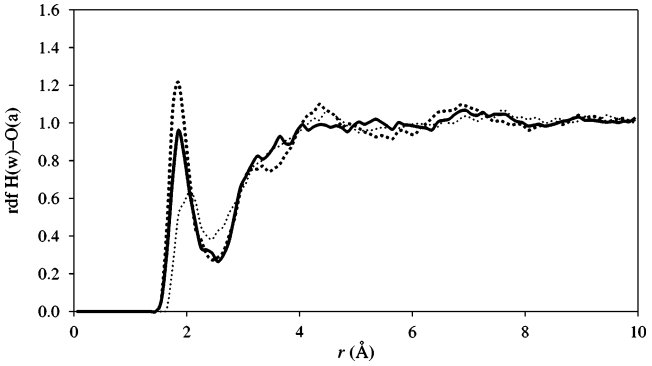

Figure 6. Oxygen(acrolein)−hydrogen(water) radial distribution functions for S_0 minimum, T_1/S_0 STC (thick lines, continuous and dotted, respectively), and S_1/S_0 CI (thin dotted line).

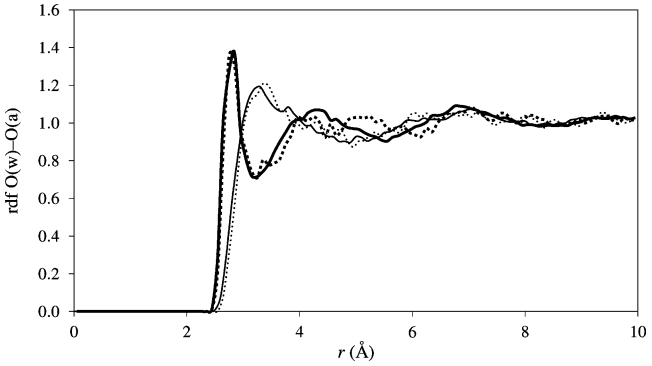

Figure 7. Oxygen(acrolein)−oxygen(water) radial distribution functions for S_0 and T_1 minima (thick lines, continuous and dotted, respectively) and S_1 and T_2 minima (thin lines, continuous and dotted, respectively).

calculated emission energy for this band is 2.24 eV, the experimental value is 2.46 eV. The solvent shift is 0.73 kcal/mol, similar to that found in the fluorescence spectrum.[24]

The different crossing points have also been located for a frozen solvent situation. Depending on the case, the search procedure can be more complicated than in the equilibrium solvation situation; see Figure 8. In frozen solvent conditions all of the crossing points are less stable than the corresponding equilibrium points. So, for instance, the S_1/S_0 CI is 6.3 kcal/mol above the FC point. However, the path that involves the S_1/T_1 and T_1/S_0 STC is still energetically possible. This path does not imply solvent reorganization, only solute movements, and hence can take place, in principle, at practically the same speed as in vacuo and must be faster than the corresponding equilibrium path. In conclusion, the radiationless relaxation of

Figure 8. Evolution during the search procedure of the S_0 and S_1 energies (in hartree) in nonequilibrium conditions (thin lines, continuous and dotted, respectively) and in equilibrium conditions (thick lines, continuous and dotted, respectively).

acrolein in aqueous solution could follow the same path as that of the in vacuo system and proceed with a similar speed.

V. Conclusions

A new method to locate minimum energy points of CI and STC in solution has been presented. The method permits us to combine high level quantum calculations in the solute description with a detailed description of the solvent structure obtained from molecular dynamics simulations. Furthermore, the method can be used with the solvent in equilibrium and nonequilibrium conditions. As an example of application, we have studied the radiationless de-excitation of s-*trans*-acrolein which involves several IC and ISC processes.

In acrolein, the solvent does not introduce drastic changes in the geometries of CI and STC points. Furthermore, the small changes found are completely similar to those found for minima. The solvent modifies the relative stability of the different CI and STC but not enough as to alter the order of stability. Consequently, the radiationless relaxation of acrolein in aqueous solution can follow the same path as in vacuo. This is valid both for equilibrium and for nonequilibrium solvent conditions. However, the relaxation through an equilibrium path involves a strong solvent reorganization; hence, this path will be slower than the in vacuo path. On the contrary, the nonequilibrium path does not involve solvent motion, and the de-excitation can proceed with the same speed as in vacuo.

Acknowledgment. This work was supported by the CTQ2004-05680 Project from the Ministerio de Educación y Ciencia of Spain.

References and Notes

(1) Yarkony, D. R. In *Conical Intersections, Advanced Series in Physical Chemistry*; Domcke, W., Yarkony, D. R., Köppel, H., Eds.; World Scientific: Singapore, 2004; Chapter 2, No. 15, p 41.

(2) Olivucci, M.; Sinicropi, A. In *Computational Photochemistry, Theoretical and Computational Chemistry;* Olivucci, M., Ed.; Elsevier: Amsterdam, 2005; Chapter I, No. 16, p 1.

(3) Yarkony, D. R. *J. Chem. Phys.* **1990**, *92*, 2457.

(4) Atchity, G. J.; Xantheas, S. S.; Ruedenberg, K. *J. Chem. Phys.* **1991**, *95*, 1862.

(5) (a) Reguero, M.; Olivucci, M.; Bernardi, F.; Robb, M. A. *J. Am. Chem. Soc.* **1994**, *116*, 2103. (b) Ragazos, N.; Robb, M. A.; Bernardi, F.; Olivucci, M. *Chem. Phys. Lett.* **1992**, *197*, 217.

(6) Burghardt, I.; Cederbaum, L.; Hynes, J. T. *Faraday Discuss.* **2004**, *127*, 395.

(7) Spezia, R.; Burghardt, I.; Hynes, J. T. *Mol. Phys.* **2006**, *104*, 903.

(8) Yamazaki, S.; Kato, S. *J. Chem. Phys.* **2005**, *123*, 114510.

(9) (a) Toniolo, A.; Granucci, G.; Martínez, T. J. *J. Phys. Chem. A* **2003**, *107*, 3822. (b) Toniolo, A.; Ben-Nun, M.; Martínez, T. J. *J. Phys. Chem. A* **2002**, *106*, 4679.

(10) (a) Garavelli, M.; Rugen, F.; Ogliano, F.; Bearpark, M. J.; Bernardi, F.; Olivucci, M.; Robb, M. A. *J. Comput. Chem.* **2003**, *24*, 1357. (b) Frutos, L. M.; Andruniów, T.; Santoro, F.; Ferré, N.; Olivucci, M. *Proc. Natl. Acad. Sci. U.S.A.* **2007**, *104*, 7764.

(11) Ciminelli, C.; Granucci, G.; Persico, *M. Chem. Eur. J.* **2004**, *10*, 2327.

(12) Bearpark, M. J.; Robb, M. A; Schlegel, H. B. *Chem. Phys. Lett.* **1994**, *223*, 269.

(13) (a) Fdez. Galván, I.; Sánchez, M. L.; Martín, M. E.; Olivares del Valle, F. J.; Aguilar, M. A. *Comput. Phys. Commun.* **2003**, *155*, 244. (b) Sánchez, M. L.; Martín, M. E.; Aguilar, M. A.; Olivares del Valle, F. J. *J. Comput. Chem.* **2000**, *21*, 705. (c) Martín, M. E.; Sánchez, M. L.; Olivares del Valle, F. J.; Aguilar, M. A. *J. Chem. Phys.* **2002**, *116*, 1613. (d) Sánchez, M. L.; Martín, M. E.; Fdez. Galván, I.; Olivares del Valle, F. J.; Aguilar, M. A. *J. Phys. Chem. B* **2002**, *106*, 4813.

(14) (a) Sánchez, M. L.; Aguilar, M. A.; Olivares del Valle, F. J. *J. Comput. Chem.* **1997**, *18*, 313. (b) Fdez. Galván, I.; Sánchez, M. L.; Martín, M. E.; Olivares del Valle, F. J.; Aguilar, M. A. *J. Chem. Phys.* **2003**, *118*, 255.

(15) (a) Okuyama-Yoshida, N.; Nagaoka, M.; Yamabe, T. *Int. J. Quantum Chem.* **1998**, *70*, 95. (b) Okuyama-Yoshida, N.; Kataoka, K.; Nagaoka, M.; Yamabe, T. *J. Chem. Phys.* **2000**, *113*, 3519. (c) Hirao, H.; Nagae, Y.; Nagaoka, M. *Chem. Phys. Lett.* **2001**, *348*, 350.

(16) (a) Chirlian, L. E.; Francl, M. M. *J. Comput. Chem.* **1987**, *8*, 894. (b) Breneman, C. M.; Wiberg, K. B. *J. Comput. Chem.* **1990**, *11*, 316.

(17) Fdez. Galván, I.; Martín, M. E.; Aguilar, M. A. *J. Comput. Chem.* **2004**, *25*, 1227.

(18) Kollman, P. A. *Chem. Rev.* **1993**, *93*, 2395.

(19) Frisch, M. J.; Trucks, G. W.; Schlegel, H. B.; Scuseria, G. E.; Robb, M. A.; Cheeseman, J. R.; Zakrzewski, V. G.; Montgomery, J. A., Jr.; Stratmann, R. E.; Burant, J. C.; Dapprich, S.; Millam, J. M.; Daniels, A. D.; Kudin, K. N.; Strain, M. C.; Farkas, O.; Tomasi, J.; Barone, V.; Cossi, M.; Cammi, R.; Mennucci, B.; Pomelli, C.; Adamo, C.; Clifford, S.; Ochterski, J.; Petersson, G. A.; Ayala, P. Y.; Cui, Q.; Morokuma, K.; Malick, D. K.; Rabuck, A. D.; Raghavachari, K.; Foresman, J. B.; Cioslowski, J.; Ortiz, J. V.; Stefanov, B. B.; Liu, G.; Liashenko, A.; Piskorz, P.; Komaromi, I.; Gomperts, R.; Martin, R. L.; Fox, D. J.; Keith, T.; Al-Laham, M. A.; Peng, C. Y.; Nanayakkara, A.; Gonzalez, C.; Challacombe, M.; Gill, P. M. W.; Johnson, B. G.; Chen, W.; Wong, M. W.; Andres, J. L.; Head-Gordon, M.; Replogle, E. S.; Pople, J. A. *Gaussian 98*, revision A11.3; Gaussian, Inc.: Pittsburgh, PA, 1998.

(20) Refson, K. *Comput. Phys. Commun.* **2000**, *126*, 310.

(21) Jorgensen, W. L.; Maxwell, D. S.; Tirado-Rives, J. *J. Am. Chem. Soc.* **1996**, *117*, 11225.

(22) Jorgensen, W. L.; Chandrasekhar, J.; Madura, J. D.; Impey, R. W.; Klein, M. L. *J. Chem. Phys.* **1983**, *79*, 926.

(23) Moskvin, A. E. *Theor. Exp. Chem.* **1966**, *2*, 175.

(24) Muñoz Losa, A.; Fdez. Galván, I.; Aguilar, M. A.; Martín, M. E. *J. Phys. Chem B* **2007**, *111*, 9864.